IEEE Access
Multidisciplinary : Rapid Review : Open Access Journal

Received 26 February 2024, accepted 11 March 2024, date of publication 19 March 2024, date of current version 25 March 2024.

Digital Object Identifier 10.1109/ACCESS.2024.3377907

RESEARCH ARTICLE

An Adaptive Robust Hybrid Force/Position Control for Robot Manipulators System Subject to Mismatched and Matched Disturbances

CHENGXING LV[1], **GANG CHEN**[1], **HUAMIN ZHAO**[1], **JIAN CHEN**[1], **AND HAISHENG YU**[2]

[1]School of Information and Control Engineering, Qingdao University of Technology, Qingdao 266001, China
[2]School of Automation, Qingdao University, Qingdao 266071, China

Corresponding author: Haisheng Yu (yu.hs@163.com)

This work was supported in part by the Natural Science Foundation of Shandong Province of China under Grant ZR2023MF032, Grant ZR2021MF005, and Grant ZR2023MF017; in part by the Focus on Research and Development Plan of Shandong Province of China (Major Scientific and Technological Innovation Project) under Grant 2022CXGC010608; in part by the Key Technological and Demonstration Project of Qingdao of China under Grant 23-1-2-qljh-6-gx; in part by Qingdao Natural Science Foundation under Grant 23-2-1-154-zyyd-jch; and in part by the National Natural Science Foundation of China under Grant 62273189.

ABSTRACT A novel adaptive robust hybrid force/position control (ARHFPC) strategy is proposed for robot manipulator systems subject to dynamic uncertainties and unknown matched and mismatched disturbances under input saturation. First, the position controller is designed based on the backstepping approach. The first-order low-pass filter and the auxiliary dynamic system are synthesized into the controller to overcome the complex derivative operation of virtual control and handle the effect of input saturation, respectively. Radial basis function neural networks (RBFNNs) are utilized to approximate the dynamic uncertainties and matched disturbances. Then, a disturbance observer is designed for the mismatched disturbances. To enhance control accuracy of the interaction force between the end-effector and the external environment, a fuzzy proportional-integral (FPI) control scheme is presented. Theoretical analysis proves that all signals in the closed-loop control system of robot manipulators are locally uniformly ultimately bounded (UUB). Simulation results demonstrate the effectiveness and robustness of the proposed control scheme.

INDEX TERMS Mismatched disturbances observer, input saturation, auxiliary dynamic system, robot manipulators.

I. INTRODUCTION

Over the past decades, robot manipulators have been widely employed in industrial fields [1], [2], such as handling, welding, assembling, etc. However, robotic manipulator systems are affected by the presence of matched and mismatched disturbances, dynamic uncertainties, and input saturation. Enhancing the trajectory tracking performance accuracy and the accuracy of interaction force control for the end-effector of robot manipulators remains a challenge, especially when these systems are subjected to external disturbances such as position sensor faults, mechanical vibrations, and other external disturbances.

Various nonlinear control methods have been developed to enhance the position and force tracking performance for the trajectory tracking problem of robot manipulator systems, such as sliding mode control (SMC), backstepping control, and computed torque control (CTC) [3], [4], [5], [6]. An adaptive neuron-fuzzy controller for an industrial robot manipulator is proposed to achieve the hybrid force/position control [7]. In paper [8], a new generalized proportional integral observer is designed to estimate velocity and force to achieve the robot manipulator's adaptive force/ position control. Lutscher et al. [9] proposed an indirect force controller to deal with unknown environments, providing

The associate editor coordinating the review of this manuscript and approving it for publication was Yang Tang.

intuitive control over hybrid force and positioning tasks in joint space and workspace. Wang et al. [10] proposed an adaptive fuzzy computed torque controller based on the workspace of a robot manipulator to enhance the accuracy of force control in unknown environments. In paper [11], an extended adaptive fuzzy SMC is presented for position/force control for Stewart manipulator. For reconfigurable manipulators subject to time-varying constraints, Cao et al. [12] developed an RBFNNs-based terminal SMC to achieve the hybrid force/position control. The paper [13] presents a force/position control scheme with environmental compliance for a continuum robot that allows the end position to be modified by changes in the continuum robot and environment. In paper [14], an adaptive fuzzy SMC is developed which requires the minimum dynamic information and does not need uncertainties bounds for the robot manipulators operating in uncertain environments. Peng et al. [15] proposed a neural network-based joint velocity observer to accomplish velocity-free measurement tracking control of a robot manipulator. In paper [16], an adaptive SMC is presented for a crawler-type mobile manipulator to realize the force/position control. Yang et al. [17] developed a RBFNNs-based adaptive impedance controller for tracking the expected interaction force, and the joint velocity is estimated by a nonlinear velocity observer. To the best of our knowledge, there are few controller strategies have been discussed to enhance the control accuracy of the robot manipulators with mismatched disturbances.

The tracking performance of robot manipulators is always influenced by actuator faults, uncertainties and external disturbances. The disturbances are generally composed of the matched and mismatched disturbances [18], [19], [20], [21]. Matched disturbances directly hold up the system states of robot manipulators through the control input. It usually contains the friction of joints. In contrast, mismatched disturbances indirectly affect the system states of the robot manipulators in the absence of control inputs. Mismatched disturbances widely present in some real engineering system. While the mismatched disturbances usually contain the nonlinear terms in rotational kinematic, actuator failure, and external environmental disturbances. As a result, the robot may fail to perform tasks precisely or may exhibit undesired behavior, such as overshooting or oscillations. How to design the control scheme to eliminate the effect of mismatched disturbances is still a challenge.

Disturbance observer is commonly employed to achieve high-performance tracking control in robot manipulators [22]. Several studies [23], [24], [25] have focused on constructing disturbance observers to estimate mismatched disturbances presumed to originate from an exogenous system. To reduce the influence of mismatched uncertainties, a self-learning disturbance observer-based feedback linearization controller is proposed [26]. In paper [27] and [28], a finite-time disturbance observer is proposed for mismatched disturbances. In paper [29] and [30], an adaptive disturbance observer is presented. Zhou et al. [31] investigated the tracking control for strict-feedback nonlinear system under mismatched disturbances. A backstepping controller is designed, and the disturbance estimates are inserted in the virtual control for mismatched disturbances rejection. However, other significant factors such as dynamic uncertainties and input saturation have not been fully considered in these studies.

In some industrial applications, the force/position tracking performance has to be as accurate as feasible. This requires the ability to accurately approximate external disturbances and dynamic uncertainties. Consequently, this work proposes a robust hybrid force/position control strategy for robot manipulators with matched and mismatched disturbances, dynamic uncertainties under input saturation. The proposed controller can track trajectories precisely and reinforce the precision of the end-effector's interaction force control. The contributions of this work are composed mainly of the following:

- A novel adaptive robust hybrid force/position control (ARHFPC) strategy is proposed for robot manipulator systems subject to unknown matched and mismatched disturbances, dynamic uncertainties and input saturation. A disturbance observer is designed for the tracking control of robot manipulators subject to mismatched disturbances. LuGre friction model is described the friction dynamics. The observer ensures that the estimation error remains bounded and converges to a neighborhood near the origin.
- RBFNNs with a new adaptive law are used to approximate the dynamic uncertainties. The proposed controller scheme can simultaneously handle dynamic uncertainties and input saturation for the trajectory tracking of robot manipulators under unknown time-varying disturbances.
- The fuzzy inference system is applied to improve the traditional proportional-integral force controller and enhance the precision of the interaction force control.

This paper is organized as follows. Section II addresses the dynamic model of robot manipulators under mismatched and matched disturbances, uncertainties and input saturation. In Section III, the design process of the position/force controller based on backstepping and fuzzy techniques is introduced. Stability analysis is given in Section IV. The simulation results are provided in Section V. Conclusions are given in Section VI.

II. PROBLEM STATEMENT

A. DYNAMIC MODEL OF ROBOT MANIPULATOR SYSTEM

The dynamic model of the n-rigid link serial robot manipulator is described by:

$$M(q)\ddot{q} + C(q,\dot{q})\dot{q} + G(q) + \tau_d + F_f(\dot{q}) = \tau + J^{\mathrm{T}}\lambda. \tag{1}$$

where $M(q) \in \mathbb{R}^{n\times n}$ denotes the inertia matrix, $C(q,\dot{q}) \in \mathbb{R}^{n\times n}$ denotes the Coriolis and Centrifugal force matrix, and $G(q) \in \mathbb{R}^n$ represents the gravitation torque. $q = [q_1, \cdots, q_n]^{\mathrm{T}} \in \mathbb{R}^n$, $\dot{q} \in \mathbb{R}^n$, $\ddot{q} \in \mathbb{R}^n$ represent the positions, velocities, and accelerations vectors. $\tau = [\tau_1, \cdots, \tau_n]^{\mathrm{T}} \in \mathbb{R}^n$ is the actual input vector. $\tau_d = [\tau_{d1}, \cdots, \tau_{dn}]^{\mathrm{T}} \in \mathbb{R}^n$ represents the matched disturbance vector. $F_f(\dot{q}) = \left[F_{f1}, \cdots, F_{fn}\right]^{\mathrm{T}} \in \mathbb{R}^n$ represents the joint friction vector. $\lambda \in \mathbb{R}^m$ represents the interaction force. $J \in \mathbb{R}^{m\times n}$ denotes the Jacobian matrix. LuGre friction model [32] is defined to described the friction dynamics

$$F_f = \varphi_1 \left(\tanh\left(\gamma_1 \dot{q}\right) - \tanh\left(\gamma_2 \dot{q}\right)\right) + \varphi_2 \tanh\left(\gamma_3 \dot{q}\right) + \varphi_3 \dot{q}\,, \tag{2}$$

where $\gamma_1, \gamma_2, \gamma_3, \varphi_1, \varphi_2, \varphi_3$ are positive parameters.

Assumption 1: The friction vector and unknown time-varying disturbance are bounded:

$$\left\|F_f(\dot{q})\right\| \le a_1 + a_2 \left\|(\dot{q})\right\|, \left\|\tau_d\right\| \le a_3. \tag{3}$$

where a_1, a_2, a_3 are positive constants.

The disturbances are generally composed of the matched and mismatched disturbances. Mismatched disturbances are those that not in the same channel as the control input. The matched disturbances are those that in the same channel as the control input. Then, we can rewritten the dynamics model (1) with matched and mismatched disturbances as the following joint-space form

$$\begin{cases} \dot{x}_1 = x_2 + d(t) \\ \dot{x}_2 = \Xi(x_1, x_2) + \Psi(x_1, x_2)\,\tau + \Theta(x_2, t) \\ y = x_1 \end{cases} \tag{4}$$

where the state vectors $x_1 \in \mathbb{R}^n$ and $x_2 \in \mathbb{R}^n$ represent the joint positions and velocities, respectively, and $\Xi(x_1, x_2) = -M^{-1}(q)\left(C(q,\dot{q})\,\dot{q} + G(q)\right)$, $\Psi(x_1,x_2) = M^{-1}(q)$, $\Theta(x_2,t) = -M^{-1}(q)\left(\tau_d + F_f\right)$. $d(t) = [d_1, \cdots, d_n]^{\mathrm{T}} \in \mathbb{R}^n$ represents the unknown time-varying mismatched disturbance.

Assumption 2: The disturbances $d(t)$ are bounded, and the condition $\lim_{t\to\infty} \dot{d}(t) = 0$ holds.

For the subsequent work, the dynamic model of the robot manipulator should have the following properties.

Property 1: $M(q)$ is a symmetric and positive definite invertible matrix. There exists with the positive constants c_1, c_2 satisfying the following conditions:

$$c_1 \left\|e\right\|^2 \le e^T M(q)\, e \le c_2 \left\|e\right\|^2, \quad \forall e \in \mathbb{R}^n. \tag{5}$$

Property 2: $\dot{M}(q) - 2C(\dot{q}, q)$ is a skew-symmetric matrix,

$$e^T \left[\dot{M}(q) - 2C(\dot{q}, q)\right] e = 0, \quad \forall e \in \mathbb{R}^n. \tag{6}$$

The precise dynamic parameters such as the inertia and the Coriolis and Centrifugal force is difficult to obtain in practice due to measurement errors and environmental factors. Therefore, the terms $M(q)$, $C(q,\dot{q})$, $G(q)$ are divided into the nominal terms $M_0(q)$, $C_0(q,\dot{q})$, $G_0(q)$ and the uncertain terms $\Delta M(q)$, $\Delta C(q,\dot{q})$, $\Delta G(q)$, respectively. It can be described as

$$\begin{cases} M(q) = M_0(q) + \Delta M(q) \\ C(q,\dot{q}) = C_0(q,\dot{q}) + \Delta C(q,\dot{q}) \\ G(q) = G_0(q) + \Delta G(q)\,. \end{cases} \tag{7}$$

Assumption 3: The uncertain terms are bounded

$$\left\|\Delta M(q)\right\| \le \ell_M, \quad \left\|\Delta C(q,\dot{q})\right\| \le \ell_C, \quad \left\|\Delta G(q)\right\| \le \ell_G\,, \tag{8}$$

where ℓ_M, ℓ_C, ℓ_G are positive constants.

B. INPUT SATURATION

Taking into account the physical limitations of the robot manipulator's joint motors, the control input is subject to the input saturation

$$\tau = \begin{cases} \tau_{\max}, & \text{if} \quad \tau_c \ge \tau_{\max} \\ \tau_c, & \text{if} \quad \tau_{\min} < \tau_c < \tau_{\max} \\ \tau_{\min}, & \text{if} \quad \tau_c \le \tau_{\min}\,, \end{cases} \tag{9}$$

where $\tau_{\max} = [\tau_{1,\max}, \cdots, \tau_{n,\max}]^{\mathrm{T}}$ is the maximum control force or moment and $\tau_{\min} = [\tau_{1,\min}, \cdots, \tau_{n,\min}]^{\mathrm{T}}$ is the minimum control force or moment provided by motors, respectively.

C. NEURAL NETWORK FUNCTION APPROXIMATION

As neural networks are excellent at approximating nonlinear functions, the nonlinear terms of the robot manipulator are approximated by the RBFNNs. The form of RBFNNs is given as:

$$F(Z) = W^{\mathrm{T}} S(Z)\,, \tag{10}$$

where $F(Z): \mathbb{R}^q \to \mathbb{R}$ represents a nonlinear function, $Z = \left[Z_1, \cdots, Z_q\right]^{\mathrm{T}} \in \mathbb{R}^q \in \Omega_Z$ denotes the input of the neural network, $W = [w_1, \cdots, w_l]^{\mathrm{T}} \in \mathbb{R}^l$ rpesents the weight vector, $l > 1$ describes the network node number, and $S(Z) = [s_1, \cdots, s_l]^{\mathrm{T}} \in \mathbb{R}^l$ represents the Gaussian basis function

$$s_i(Z) = \exp\left(\frac{-(Z-\beta_i)^{\mathrm{T}}(Z-\beta_i)}{\eta_i^2}\right), \quad i = 1, 2, \cdots, l\,, \tag{11}$$

where η_i and $\beta_i = [\beta_{i1}, \cdots, \beta_{iq}]^{\mathrm{T}}$ are the width and centers of the Gaussian function, respectively.

The equation (10) can be described as follows

$$F(Z) = W^{*\mathrm{T}} S(Z) + \Delta\,, \tag{12}$$

where Δ expressed as the error of approximation, which satisfies $|\Delta| \le \bar{\Delta}$ with $\bar{\Delta} > 0$ being a constant. W^* represents an ideal constant weight which can described as

$$W^* = \arg\min_{W\in\mathbb{R}^q} \left\{ \sup_{Z\in\Omega_Z} \left| F(Z) - W^{\mathrm{T}} S(Z) \right| \right\}. \tag{13}$$

Control Objective: This paper aims to propose an adaptive robust hybrid force/position controller for the robot manipulator system described by equation (1) with matched and mismatched disturbances, uncertainties and input saturation such that the closed-loop system is bounded under Assumptions 1-3. The hybrid controller is expected to exhibit excellent tracking performance, as evidenced by the convergence of the tracking error $\lim_{t\to\infty} \tilde{x}_1, \tilde{\lambda} \to 0$.

III. DESIGN OF ADAPTIVE ROBUST HYBRID FORCE/POSITION CONTROLLER

In this section, we develop a novel Adaptive Robust Hybrid Force/Position Control (ARHFPC) scheme for the robot manipulator, aiming to enhance both trajectory tracking performance and the accuracy of the end-effector's interaction force control. The proposed controller comprises several key components: a low-pass filter, a backstepping controller, Radial Basis Function Neural Networks (RBFNNs), a Mismatched Disturbance Observer (MDO), an Auxiliary Dynamic System (ADS), and a Fuzzy Inference System (FIS). The low-pass filter is employed to address the complex derivation problem of the virtual control input. RBFNNs are utilized to approximate dynamic uncertainties, while the MDO is constructed to reject mismatched disturbances. Additionally, an ADS is employed to mitigate the effects of input saturation. Furthermore, a FIS system is applied to enhance the traditional proportional-integral force controller and improve the accuracy of interaction force control. Figure 1 illustrates the structure of the proposed control scheme.

A. POSITION CONTROLLER DESIGN

The position controller is developed step by step using the backstepping technique. Firstly, some auxiliary variables is introduced. Then, the candidate Lyapunov function is presented directly..

Step 1: The state error is defined as:

$$\tilde{x}_1 = x_1 - x_d\,, \tag{14}$$

where x_d is the desired trajectory. The derivative of the state error (13) is defined as

$$\dot{\tilde{x}}_1 = \alpha - \dot{x}_d\,, \tag{15}$$

and the virtual control input is defined as

$$\alpha = -K_1\tilde{x}_1 + \dot{x}_d - \hat{d}\,(t)\,, \tag{16}$$

where $\hat{d}\,(t)$ represents the estimation of $d\,(t)$. The Lyapunov function candidate is defined as

$$V_1 = \frac{1}{2}\tilde{x}_1^T\tilde{x}_1\,. \tag{17}$$

The following low-pass filter with time constant T_0 is applied:

$$\begin{cases} T_0\dot{\upsilon}_d + \upsilon_d = \alpha \\ \upsilon_d(0) = \alpha(0)\,, \end{cases} \tag{18}$$

where υ_d denotes the state of the filter, and $\dot{\upsilon}_d$ which is used to replace the $\dot{\alpha}$ can be obtained directly from the filter.

Step 2: Define the state error as:

$$\tilde{x}_2 = x_2 - \upsilon_d\,, \tag{19}$$

Therefore, differentiating the Lyapunov function V_1, we can obtain

$$\begin{aligned}\dot{V}_1 &= -\tilde{x}_1^T\dot{\tilde{x}}_1 \\ &= -\tilde{x}_1^TK_1\tilde{x}_1 + \tilde{x}_1^T\tilde{x}_2,\end{aligned} \tag{20}$$

The Lyapunov candidate function is defined as follows:

$$V_2 = V_1 + \frac{1}{2}\tilde{x}_2^TM\tilde{x}_2. \tag{21}$$

According to Property 2, the time derivative of V_2 can be described as:

$$\begin{aligned}\dot{V}_2 &= -\tilde{x}_1^TK_1\tilde{x}_1 + \tilde{x}_1^T\tilde{x}_2 + \frac{1}{2}\tilde{x}_2^T(\dot{M} - 2C)\tilde{x}_2 \\ &\quad + \tilde{x}_2^T(\tau - \tau_d - F_f - C\upsilon_d - G - M\dot{\upsilon}_d) \\ &= -\tilde{x}_1^TK_1\tilde{x}_1 + \tilde{x}_1^T\tilde{x}_2 + \tilde{x}_2^T(\tau - \tau_d - F_f \\ &\quad - C\upsilon_d - G - M\dot{\upsilon}_d).\end{aligned} \tag{22}$$

To handle the dynamic uncertainties, matched disturbances, and joint friction, the RBFNNs are used to approximate

$$W^{*T}S(Z) = \Delta M\dot{\upsilon}_d + \Delta C\upsilon_d + \Delta G + \tau_d + F_f + \varepsilon(Z)\,, \tag{23}$$

where $Z = [q^T, \dot{q}^T, \upsilon_d{}^T, \dot{\upsilon}_d^T]^T \in \Omega_Z$, $\varepsilon(Z)$ denotes the approximate error vector and satisfies $\|\varepsilon(Z)\| \leq \bar{\varepsilon}$. Define $\hat{W}$ as an estimation of W^*, the estimation error is $\tilde{W} = W^* - \hat{W}$. Therefore, the following controller is designed

$$\tau_s = C_0\upsilon_d + G_0 + M_0\dot{\upsilon}_d - \tilde{x}_1 - K_2\tilde{x}_2 + \hat{W}^TS(Z)\,, \tag{24}$$

with the adaptive law:

$$*20c\dot{\hat{W}}_i = -P_i(S_i(Z)\tilde{x}_{2,i} + \sigma_i\hat{W}_i), i = 1, \cdots, n\,, \tag{25}$$

where $P_i > 0$ and $\sigma_i > 0$ are design parameters.

The following ADS is formed to settle the influence of input saturation [33]:

where $\Delta\tau = \tau - \tau_c$, $\vartheta = [\vartheta_1, \cdots, \vartheta_n]^T \in \mathbb{R}^n$ represents the state vector, $K_0 = K_0^T \in \mathbb{R}^{n\times n}$ represents a positive parameter matrix and $\omega > 0$ denotes a small positive scalar.

Therefore, combining equation (24) and (26), as shown at the bottom of the next page, the position controller is proposed as follows

$$\tau_c = \tau_s + \tau_a\,, \tag{27}$$

where $\tau_a = K_a\vartheta$, $K_a \in \mathbb{R}^{n\times n}$ is described as a positive gain matrix.

According equation (27), we can rewritten the equation (22) as follow

$$\begin{aligned}\dot{V}_2 &= -\tilde{x}_1^TK_1\tilde{x}_1 - \tilde{x}_2^TK_2\tilde{x}_2 + \tilde{x}_2^T\tilde{W}^TS(Z) \\ &\quad + \tilde{x}_2^T\varepsilon(Z) + \tilde{x}_2^TK_a\vartheta\,,\end{aligned} \tag{28}$$

where $K_1 = diag\,[k_{11}, \cdots, k_{1n}]$ and $K_2 = diag\,[k_{21}, \cdots, k_{2n}]$ are design positive parameter matrices.

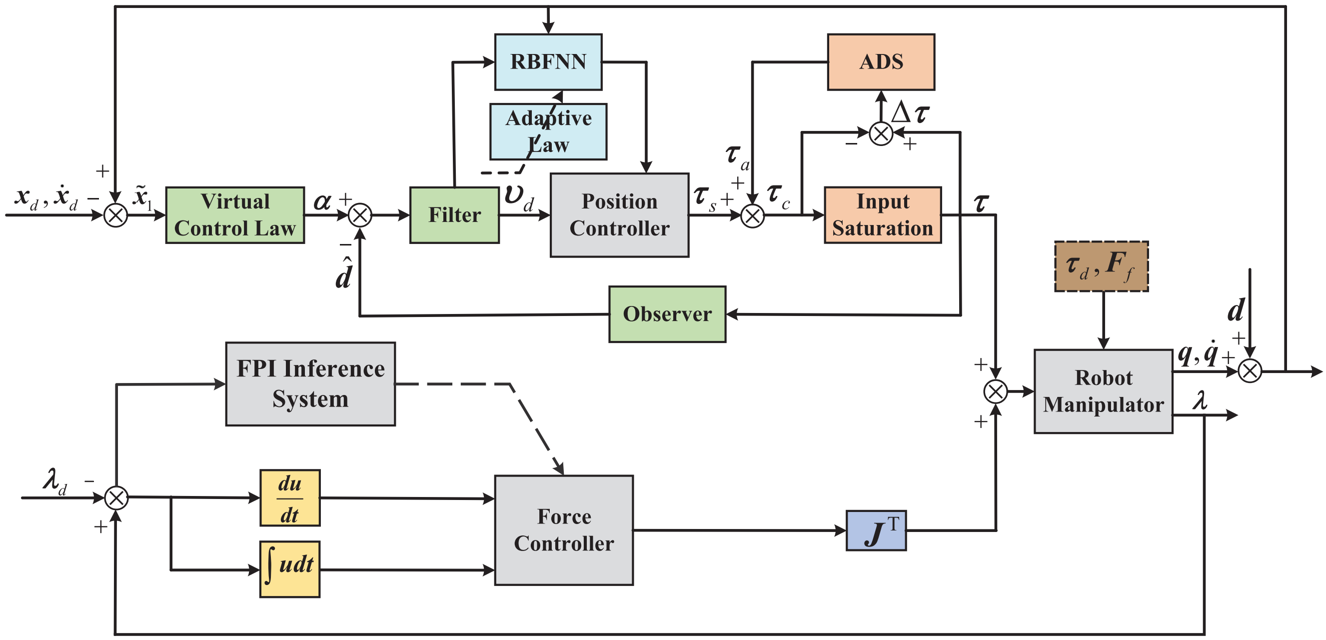

FIGURE 1. Scheme of the adaptive robust hybrid force/position controller for robot manipulator.

B. MISMATCHED DISTURBANCE OBSERVER DESIGN

The time derivative of the state error (14) is:

$$\dot{\tilde{x}}_1 = \dot{x}_1 - \dot{x}_d = x_2 + d - \dot{x}_d. \tag{29}$$

Substituting equation (4) into equation (29), we obtain

$$\begin{aligned}\ddot{\tilde{x}}_1 &= \dot{x}_2 + \dot{d} - \ddot{x}_d \\ &= \Xi(x_1, x_2) + \Psi(x_1, x_2)\tau + \dot{d} - \ddot{x}_d \\ &= \Gamma(x_1, x_2, x_d) + \Psi(x_1, x_2)\tau + \dot{d}\,,\end{aligned} \tag{30}$$

where $\Gamma(x_1, x_2, x_d) = \Xi(x_1, x_2) - \ddot{x}_d$.

The following observer is proposed for rejecting the influence of mismatched disturbance

$$\begin{cases}\hat{d} = \delta + N \\ \dot{\delta} = -L(\Gamma(x_1, x_2, x_d) + \Psi(x_1, x_2)\tau) - L\hat{d}\,,\end{cases} \tag{31}$$

where $N = L\dot{\tilde{x}}_1$, $\delta \in \mathbb{R}^n$ represents the state vector of the observer, and $L = \mathrm{diag}[l_1, \cdots, l_n]$ is a positive gain matrix. Define the disturbance observer error as $\tilde{d} = d - \hat{d}$, and its derivative can be obtained

$$\begin{aligned}\dot{\tilde{d}} &= \dot{d} - \dot{\hat{d}} \\ &= \dot{d} - \dot{\delta} - \dot{N} \\ &= \dot{d} + L(\Gamma(x_1, x_2, x_d) + \Psi(x_1, x_2)\tau) \\ &\quad + L\hat{d} - L\ddot{\tilde{x}}_1 \\ &= \dot{d} - L\left(\dot{d} - \hat{d}\right).\end{aligned} \tag{32}$$

The Lyapunov function candidate is chosen to be

$$V_d = \frac{1}{2}\tilde{d}^{\mathrm{T}}\tilde{d}. \tag{33}$$

Taking its first time derivative, we can obtain

$$\begin{aligned}\dot{V}_d &= \tilde{d}^{\mathrm{T}}\left(\dot{d} - L\left(\dot{d} - \hat{d}\right)\right) \\ &= \tilde{d}^{\mathrm{T}}\dot{d} - \tilde{d}^{\mathrm{T}}L\dot{d} + \tilde{d}^{\mathrm{T}}L\hat{d}\,.\end{aligned} \tag{34}$$

From the following square inequality

$$\tilde{d}^{\mathrm{T}}\dot{d} \le \varepsilon_1\tilde{d}^{\mathrm{T}}\tilde{d} + \frac{1}{4\varepsilon_1}\dot{d}^{\mathrm{T}}\dot{d}, \tag{35}$$

$$-\tilde{d}^{\mathrm{T}}L\dot{d} \le -\varepsilon_2\tilde{d}^{\mathrm{T}}\tilde{d} - \frac{1}{4\varepsilon_2}\dot{d}^{\mathrm{T}}L^{\mathrm{T}}L\dot{d}, \tag{36}$$

$$\tilde{d}^{\mathrm{T}}L\hat{d} \le \varepsilon_3\tilde{d}^{\mathrm{T}}\tilde{d} + \frac{1}{4\varepsilon_3}\hat{d}^{\mathrm{T}}L^{\mathrm{T}}L\hat{d}\,, \tag{37}$$

where ε_1, ε_2, ε_3 are small positive constants. Subsequently, equation (34) can be reformed as:

$$\dot{V}_d \le -bV_d + c\,, \tag{38}$$

where

$$b = 2(\varepsilon_2 - \varepsilon_1 - \varepsilon_3), \tag{39}$$

$$c = \left(\frac{1}{4\varepsilon_1} - \frac{\lambda_{\min}(L^{\mathrm{T}}L)}{4\varepsilon_2}\right)C_d^2 + \frac{\lambda_{\min}(L^{\mathrm{T}}L)}{4\varepsilon_3}\hat{d}^T\hat{d}. \tag{40}$$

$$\dot{\vartheta} = \begin{cases}-K_0\vartheta - \dfrac{\sum_{i=1}^{n}\left|\tilde{x}_{2,i}\Delta\tau_i\right| + 0.5\Delta\tau^{\mathrm{T}}\Delta\tau}{\|\vartheta\|^2}\vartheta + \Delta\tau, & \|\vartheta\| \ge \omega \\ 0_{n\times 1}, & \|\vartheta\| < \omega\end{cases} \tag{26}$$

Then, we have $\dot{V}_d \leq 0$ by choosing the appropriate parameters. The disturbance estimation error is bounded and converges to a neighborhood near the origin.

C. FORCE CONTROLLER DESIGN

In some working scenario, the robot manipulator is tasked with trajectory tracking while simultaneously adhering to constraints on the force exerted by the end-effector due to human interaction and environmental factors. To achieve this, selection matrices S_1 and S_2 are commonly employed to designate the control mode for each joint. During the design of the force controller, we aim to keep the Z-axis interaction force λ constrained.

The force controller takes the following form:

$$\lambda = K_p^* \tilde{\lambda} + K_i^* \int \tilde{\lambda} \mathrm{d}t\,, \tag{41}$$

where $\tilde{\lambda} = \lambda - \lambda_d$ is defined as the interaction force error, λ_d is the desired force. K_p^* and K_i^* are proportional gain and integral gain, respectively.

In order to better improve the force tracking effect of the end-effector, we introduce the dynamic adjustable parameter. Then, FIS technique is utilized to adjust the parameters of the force controller. Define $\tilde{\lambda}$ and $d\tilde{\lambda}$ as the inputs of the inference system, and ΔK_p and ΔK_i represent the system outputs. The IF $\sim$ THEN rule of the FIS is designed as follows:

$$\begin{aligned} &\text{Rule} \quad R_{bc}: \quad \text{IF} \quad \tilde{\lambda}_r \quad \text{is} \quad B_b, \quad d\tilde{\lambda}_r \quad \text{is} \quad C_c, \\ &\qquad \text{THEN} \quad \Delta K_{ir} \quad \text{is} \quad r_{bc}, \quad \Delta K_{pr} \quad \text{is} \quad v_{bc}\,, \end{aligned}$$

where $r = 1, 2, \cdots, m$, $B_b(b = 1, 2, \cdots b_N)$ and $C_c(c = 1, 2, \cdots c_N)$ are the fuzzy sets for $\tilde{\lambda}_r$ and $d\tilde{\lambda}_r$. r_{bc} and v_{bc} are described as the central of fuzzy sets for ΔK_{ir} and ΔK_{pr}. Applying singleton fuzzification, product inference, and center average defuzzification, the final FIS can be obtain

$$\begin{cases} \Delta K_{ir} = \dfrac{\sum_{b=1}^{b_N} \sum_{c=1}^{c_N} \mu_{B_b}(\tilde{\lambda}_r)\mu_{C_c}(d\tilde{\lambda}_r) r_{bc}}{\sum_{b=1}^{b_N} \sum_{c=1}^{c_N} \mu_{B_b}(\tilde{\lambda}_r)\mu_{C_c}(d\tilde{\lambda}_r)} \\ \Delta K_{pr} = \dfrac{\sum_{b=1}^{b_N} \sum_{c=1}^{c_N} \mu_{B_b}(\tilde{\lambda}_r)\mu_{C_c}(d\tilde{\lambda}_r) v_{bc}}{\sum_{b=1}^{b_N} \sum_{c=1}^{c_N} \mu_{B_b}(\tilde{\lambda}_r)\mu_{C_c}(d\tilde{\lambda}_r)}\,, \end{cases} \tag{42}$$

where $\mu_{B_b}(\tilde{\lambda}_r)$ and $\mu_{C_c}(d\tilde{\lambda}_r)$ are the membership functions in the fuzzy sets B_b and C_c, respectively. Subsequently, the follow equation can be obtained:

$$\begin{cases} \hat{K}_{ir} = K_{ir0}^* + \Delta K_{ir} \\ \hat{K}_{pr} = K_{pr0}^* + \Delta K_{pr}\,, \end{cases} \tag{43}$$

where K_{ir0}^* and K_{pr0}^* are the initial values of K_{ir}^*, K_{pr}^*. $K_{i0}^* = \mathrm{diag}[K_{i10}^*, \cdots, K_{im0}^*]$, $K_{p0}^* = \mathrm{diag}\left[K_{p10}^*, \cdots, K_{pm0}^*\right]$, $\Delta K_i = \mathrm{diag}\left[\Delta K_{i1}, \cdots, \Delta K_{im}\right]$, $\Delta K_p = \mathrm{diag}\left[\Delta K_{p1}, \cdots, \Delta K_{pm}\right]$.

From equation (39), and (41), the force controller based on the FIS in Cartesian space can be described as:

$$\lambda = \hat{K}_i \int \tilde{\lambda} \mathrm{d}t + \hat{K}_p \tilde{\lambda}\,, \tag{44}$$

where $\hat{K}_i = \mathrm{diag}\left[\hat{K}_{i1}, \cdots, \hat{K}_{im}\right]$, $\hat{K}_p = \mathrm{diag}\left[\hat{K}_{p1}, \cdots, \hat{K}_{pm}\right]$. The Cartesian space force λ is converted into joint-space torque by using the Jacobian matrix

$$\tau_\lambda = J^{\mathrm{T}} S_2 \lambda. \tag{45}$$

Finally, the hybrid force/position controller is proposed as follow:

$$\tau = \tau_c + \tau_\lambda\,, \tag{46}$$

with the adaptive law (25) and fuzzy law (43). FIS Dynamic Adjustable Parameter Technology introduces force errors into parameter changes, allowing real-time adjustment of the controller's output action.

IV. STABILITY ANALYSIS

The following Lyapunov candidate function is selected for the closed-loop system

$$\begin{aligned} V = \frac{1}{2}\tilde{x}_1^{\mathrm{T}}\tilde{x}_1 + \frac{1}{2}\tilde{x}_2^{\mathrm{T}} M \tilde{x}_2 + \sum\nolimits_{i=1}^{n} \tilde{W}_i^{\mathrm{T}} P_i^{-1} \tilde{W}_i \\ + \frac{1}{2}\tilde{d}^{\mathrm{T}}\tilde{d} + \frac{1}{2}\vartheta^{\mathrm{T}}\vartheta. \end{aligned} \tag{47}$$

From equation (28), and (34), the time derivative of (47) can be obtained

$$\begin{aligned} \dot{V} &= -\tilde{x}_1^T K_1 \tilde{x}_1 - \tilde{x}_2^T K_2 \tilde{x}_2 + \tilde{x}_2^T \tilde{W}^{\mathrm{T}} S(Z) + \tilde{x}_2^T \varepsilon(Z) \\ &\quad + \tilde{x}_2^T K_a \vartheta - \sum\nolimits_{i=1}^{n} \tilde{W}_i^{\mathrm{T}} (S_i(Z)\tilde{x}_{2,i} + \sigma_i \hat{W}_i) \\ &\quad + \tilde{d}^{\mathrm{T}}\dot{d} - \tilde{d}^{\mathrm{T}} L \dot{d} + \tilde{d}^{\mathrm{T}} L \dot{\hat{d}} + \vartheta^{\mathrm{T}}\dot{\vartheta}. \end{aligned} \tag{48}$$

By using Young's inequality, we can achieve:

$$\tilde{x}_2^T \varepsilon(Z) \leq \frac{1}{2}\tilde{x}_2^T \tilde{x}_2 + \frac{1}{2}\bar{\varepsilon}^2, \tag{49}$$

$$\tilde{x}_2^T K_a \vartheta \leq \frac{1}{2}\tilde{x}_2^T \tilde{x}_2 + \frac{1}{2}\vartheta^{\mathrm{T}} K_a^{\mathrm{T}} K_a \vartheta, \tag{50}$$

$$\begin{aligned} -\sigma_i \tilde{W}_i^{\mathrm{T}} \hat{W}_i &= -\sigma_i \tilde{W}_i^{\mathrm{T}} \tilde{W}_i - \sigma_i \tilde{W}_i^{\mathrm{T}} W_i^* \\ &\leq -\frac{\sigma_i}{2}\tilde{W}_i^{\mathrm{T}}\tilde{W}_i + \frac{\sigma_i}{2} W_i^{*\mathrm{T}} W_i^*. \end{aligned} \tag{51}$$

(1) If the condition $\|\vartheta\| \geq \omega$ set, considering equation (26) and the above inequality, we have:

$$\begin{aligned} \vartheta^T \dot{\vartheta} &= -\vartheta^T K_0 \vartheta - \sum\nolimits_{i=1}^{n} \left|\tilde{x}_{2,i}\Delta\tau_i\right| - 0.5\Delta\tau^{\mathrm{T}}\Delta\tau + \vartheta^T \Delta\tau \\ &\leq -\vartheta^T (K_0\vartheta - 0.5 I_{n\times n})\vartheta - \sum\nolimits_{i=1}^{n} \left|\tilde{x}_{2,i}\Delta\tau_i\right|. \end{aligned} \tag{52}$$

Then, according to equations (35)-(37), equations (49)-(51), and equation (52), we can rewrite the equation (48) as follows:

$$\begin{aligned} &\dot{V} \\ &\leq -\tilde{x}_1^T K_1 \tilde{x}_1 - \tilde{x}_2^T K_2 \tilde{x}_2 + \tilde{x}_2^T \tilde{x}_2 + \frac{1}{2}\vartheta^{\mathrm{T}} K_a^{\mathrm{T}} K_a \vartheta \\ &\quad - \frac{\sigma_i}{2}\tilde{W}_i^{\mathrm{T}}\tilde{W}_i - (\varepsilon_2 - \varepsilon_1 - \varepsilon_3)\tilde{d}^{\mathrm{T}}\tilde{d} - \vartheta^T (K_0\vartheta \\ &\quad - 0.5 I_{n\times n})\vartheta + \frac{\sigma_i}{2} W_i^{*\mathrm{T}} W_i^* - \sum\nolimits_{i=1}^{n} \left|\tilde{x}_{2,i}\Delta\tau_i\right| \\ &\quad + \dot{d}^T (\frac{1}{4\varepsilon_1} - \frac{L^{\mathrm{T}} L}{4\varepsilon_2})\dot{d} + \dot{\hat{d}}^T \frac{L^{\mathrm{T}} L}{4\varepsilon_3}\dot{\hat{d}} + \frac{1}{2}\bar{\varepsilon}^2 \end{aligned}$$

$$\begin{aligned}&\leq -\lambda_{\min}(K_1)\tilde{x}_1^T\tilde{x}_1 - \frac{\lambda_{\min}(K_2)-1}{\lambda_{\max}(M)}\tilde{x}_2^T\tilde{x}_2 - \frac{\sigma_i}{2}\tilde{W}_i^{\mathrm{T}}\tilde{W}_i\\&\quad - (\varepsilon_2-\varepsilon_1-\varepsilon_3)\tilde{d}^{\mathrm{T}}\tilde{d} - \left[\lambda_{\min}(K_0-\frac{1}{2}K_a^{\mathrm{T}}K_a)-\frac{1}{2}\right]\vartheta^T\vartheta\\&\quad + \frac{\sigma_i}{2}W_i^{*\mathrm{T}}W_i^* + (\frac{1}{4\varepsilon_1}-\frac{\lambda_{\min}(L^{\mathrm{T}}L)}{4\varepsilon_2})C_d^2\\&\quad + \frac{\lambda_{\min}(L^{\mathrm{T}}L)}{4\varepsilon_3}\hat{d}^T\hat{d} + \frac{1}{2}\bar{\varepsilon}^2\\&\leq -\zeta_1 V + \nabla_1 \end{aligned} \tag{53}$$

where $\lambda_{\min}(\cdot)$ and $\lambda_{\max}(\cdot)$ are the matrix's minimum and maximum eigenvalues, and

$$\begin{aligned}\zeta_1 &= \min\left[2\lambda_{\min}(K_1), \frac{2\lambda_{\min}(K_2)-2}{\lambda_{\max}(M)}, -\frac{2\sigma_i}{\lambda_{\max}(P_i)},\right.\\&\qquad \left. 2(\varepsilon_2-\varepsilon_1-\varepsilon_3), \lambda_{\min}(2K_0-K_a^{\mathrm{T}}K_a)-1\right],\\\nabla_1 &= \frac{\sigma_i}{2}W_i^{*\mathrm{T}}W_i^* + (\frac{1}{4\varepsilon_1}-\frac{\lambda_{\min}(L^{\mathrm{T}}L)}{4\varepsilon_2})C_d^2\\&\qquad + \frac{\lambda_{\min}(L^{\mathrm{T}}L)}{4\varepsilon_3}\hat{d}^T\hat{d} + \frac{1}{2}\bar{\varepsilon}^2. \end{aligned} \tag{54}$$

Solving the inequality (53), we obtain:

$$0 \leq V(t) \leq \frac{\nabla_1}{\zeta_1} + \left[V(0) - \frac{\nabla_1}{\zeta_1}\right]e^{-\zeta_1 t}. \tag{55}$$

(2) If the condition $\|\vartheta\| < \omega$ set, based on (26) and Young's inequality, we have

$$\vartheta^T\dot{\vartheta} = 0\,. \tag{56}$$

According to equations (35)-(37), equations (49)-(51), and equation (56), we can rewrite the equation (48) as follows:

$$\begin{aligned}\dot{V} &\leq -\lambda_{\min}(K_1)\tilde{x}_1^T\tilde{x}_1 - \frac{\lambda_{\min}(K_2)-1}{\lambda_{\max}(M)}\tilde{x}_2^T\tilde{x}_2 - \frac{\sigma_i}{2}\tilde{W}_i^{\mathrm{T}}\tilde{W}_i\\&\quad - (\varepsilon_2-\varepsilon_1-\varepsilon_3)\tilde{d}^{\mathrm{T}}\tilde{d} + \left[\lambda_{\min}(\frac{1}{2}K_a^{\mathrm{T}}K_a)\right]\vartheta^T\vartheta\\&\quad + \frac{\sigma_i}{2}W_i^{*\mathrm{T}}W_i^* + (\frac{1}{4\varepsilon_1}-\frac{\lambda_{\min}(L^{\mathrm{T}}L)}{4\varepsilon_2})C_d^2\\&\quad + \frac{\lambda_{\min}(L^{\mathrm{T}}L)}{4\varepsilon_3}\hat{d}^T\hat{d} + \frac{1}{2}\bar{\varepsilon}^2\\&\leq -\zeta_2 V + \nabla_2\,, \end{aligned} \tag{57}$$

where

$$\begin{aligned}\zeta_2 &= \min\left[2\lambda_{\min}(K_1), \frac{2\lambda_{\min}(K_2)-2}{\lambda_{\max}(M)}, -\frac{2\sigma_i}{\lambda_{\max}(P_i)},\right.\\&\qquad \left. 2(\varepsilon_2-\varepsilon_1-\varepsilon_3), \lambda_{\min}(K_a^{\mathrm{T}}K_a)\right],\\\nabla_2 &= \frac{\sigma_i}{2}W_i^{*\mathrm{T}}W_i^* + (\frac{1}{4\varepsilon_1}-\frac{\lambda_{\min}(L^{\mathrm{T}}L)}{4\varepsilon_2})C_d^2\\&\qquad + \frac{\lambda_{\min}(L^{\mathrm{T}}L)}{4\varepsilon_3}\hat{d}^T\hat{d} + \frac{1}{2}\bar{\varepsilon}^2\,. \end{aligned} \tag{58}$$

Solving the inequality (57), we obtain:

$$0 \leq V(t) \leq \frac{\nabla_2}{\zeta_2} + \left[V(0) - \frac{\nabla_2}{\zeta_2}\right]e^{-\zeta_2 t}. \tag{59}$$

TABLE 1. Design parameters of the controllers.

Controller	Parameter	Value
ARHFPC	K_0, K_1, K_2	diag[2, 2, 2], diag[300, 300, 200], diag[300, 300, 200]
	L, T_0, K_a, l	diag[1, 1, 1], 0.01, diag[1, 1, 1], 60
	η_i, P_i, σ_i	3, 300, 0.02
	$k_e, K_{pr0}^*, K_{ir0}^*$	100, 10, 5
PD	k_p, k_d	200, 150
SMC	k_{s1}, k_{s2}	diag[10, 10, 10], diag[15, 15, 15]
Back-stepping	k_{b1}, k_{b2}	diag[50, 50, 50], diag[45, 45, 45]

TABLE 2. The fuzzy rules of ΔK_p.

ΔK_p \ $\tilde{\lambda}$ / $d\tilde{\lambda}$	N	Z	P
N	N	N	Z
Z	N	Z	P
P	Z	P	P

TABLE 3. The fuzzy rules of ΔK_i.

ΔK_i \ $\tilde{\lambda}$ / $d\tilde{\lambda}$	N	Z	P
N	N	Z	Z
Z	Z	P	P
P	Z	Z	P

Subsequently, the following theorem summarizes the main results.

Theorem 1: Consider the robot manipulator model (1) with Assumptions 1-3, the hybrid force/position controller (46) with the virtual control signal in (16), the first order filter (18), the adaptive law (25), the ADS (26), and the mismatched disturbances observer (31). If the condition $V(0) \leq C_0$ with C_0 being any positive constant hold, all the signals of the closed-loop control system remain bounded, the force and position tracking errors and observer errors remain in a neighborhood around origin.

Proof: Synthesizing equation (54) and equation (59) yield

$$0 \leq V(t) \leq \frac{\nabla}{\zeta} + \left[V(0) - \frac{\nabla}{\zeta}\right]e^{-\zeta t}\,, \tag{60}$$

where $\zeta = \min[\zeta_1, \zeta_2]$ and $\nabla = \min[\nabla_1, \nabla_2]$. According to equation (60), $V(t)$ is bounded if $V(0) \leq C_0$ hold. The Lyapunov function $V(t)$ is locally UUB. Therefore, $\tilde{x}_1$, $\tilde{x}_2$, $\tilde{W}$, $\tilde{d}$, and $\tilde{\vartheta}$ are locally UUB according to equation (47). Furthermore, the conclusion $\lim_{t\to\infty}\tilde{\lambda} = 0$ is obtained by the boundedness of q and $\dot{q}$. Therefore, the force tracking error $\tilde{\lambda}$ is also bounded and converges near a neighborhood around origin. As a result, in this closed-loop control system all signals are locally UUB. □ □ □

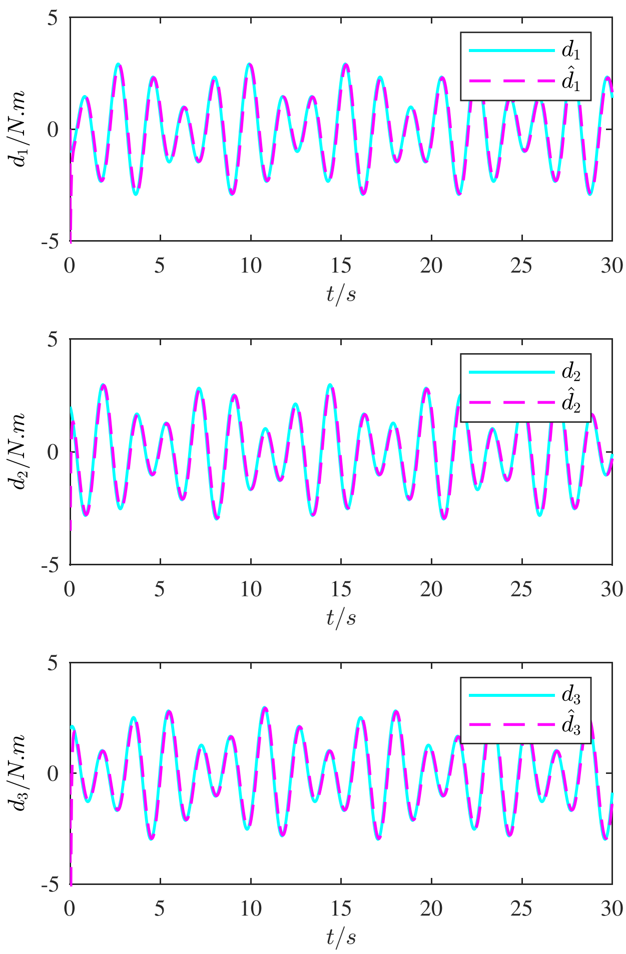

FIGURE 2. Mismatched disturbances d and their estimate values $\hat{d}$.

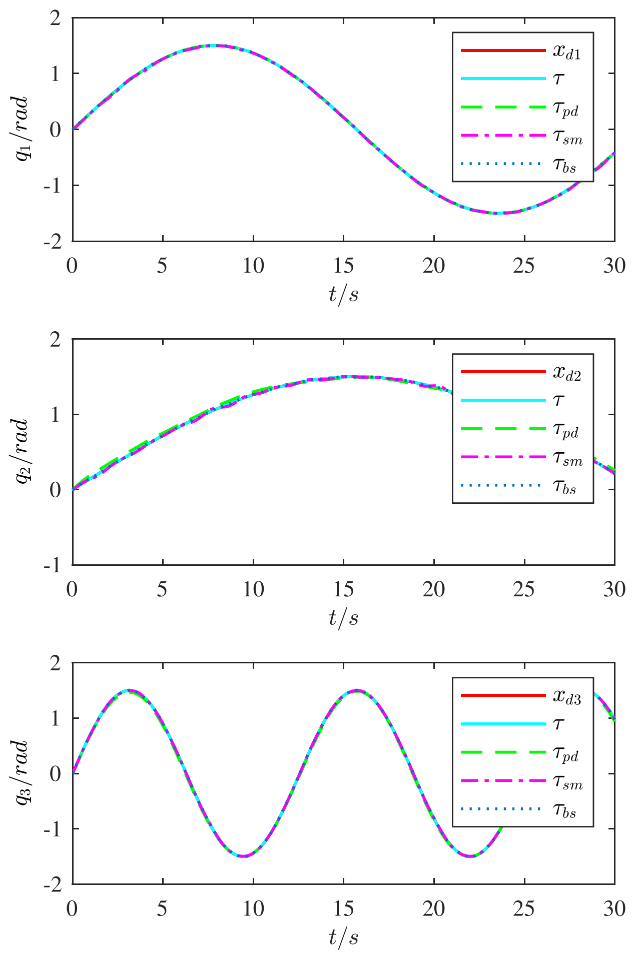

FIGURE 3. The tracking performance comparison under scenario 1.

Remark 1: Controller gains K_1, K_2 typically lead to faster error convergence, as they increase the control effort in response to the error signals $\tilde{x}_1$, $\tilde{x}_2$. The parameter K_0, K_a represents an additional control gain term. Adjusting its value can influence the control performance, particularly in situations where there are uncertainties. L terms affect the accuracy of disturbance observation and the ability of the controller to reject disturbances.

V. SIMULATION RESULTS AND DISCUSSION

The PUMA560 robot is employed to evaluate the performance of the proposed controller in this section. The first three joints is only considered for simplicity in analyzing. The detail robot parameters are given in the work [34]. The parameters of friction model (2) are chosen as $\varphi_1 = 0.2$, $\gamma_1 = 1$, $\varphi_2, \varphi_3 = 0.5$, $\gamma_2, \gamma_3 = 0.5$.

The RBFNNs' function centers β_i are evenly spaced in the range $[-2, 2] \times [-2, 2] \times [-2, 2] \times [-2, 2] \times [-2, 2] \times [-2, 2] \times [-2, 2] \times [-2, 2] \times [-2, 2] \times [-2, 2] \times [-2, 2] \times [-2, 2]$. The desired interaction force is selected as $\lambda_d = 20$N. The distance between the origin of the inertial reference frame and the Z-axis surface is considered as: $x_e = 1$m. Then, the end-effector's interaction force is described as $\lambda = k_e(x_z - x_e)$ and the selection matrix is chosen as $S_2 = \text{diag}[0, 0, 1]$, respectively.

We make a comparison to illustrate the ARHFPC controller performance with the PD controller (61), SMC controller (62), and backstepping controller (63) to illustrate the performance. All design parameters of the proposed controller are outlined in the Table 1. The joint saturation limits are set to [±50N.m, ±50N.m, ±30N.m]. In the force controller term, we define the N (negative), Z (zero), P (positive) as the fuzzy subsets, respectively. The fuzzy rules for ΔK_p and ΔK_i are presented in Table 2 and Table 3, respectively.

$$\tau_{pd} = -k_p\tilde{x}_1 - k_d\dot{\tilde{x}}_1. \tag{61}$$

$$\begin{cases} \tau_{sm} = M(\ddot{x}_d - k_{s2}\dot{\tilde{x}}_1) + C(x_2 - s) + G - k_{s2}sgn(s) \\ s = \dot{\tilde{x}}_1 + k_{s1}\tilde{x}_1. \end{cases} \tag{62}$$

$$\begin{aligned} \tau_{bs} = M\ddot{x}_d + (C - k_{b2} - Mk_{b1})x_2 + G \\ - (k_{b1}k_{b2} + I)\tilde{x}_1 + (Mk_{b1} + k_{b2})\dot{x}_d. \end{aligned} \tag{63}$$

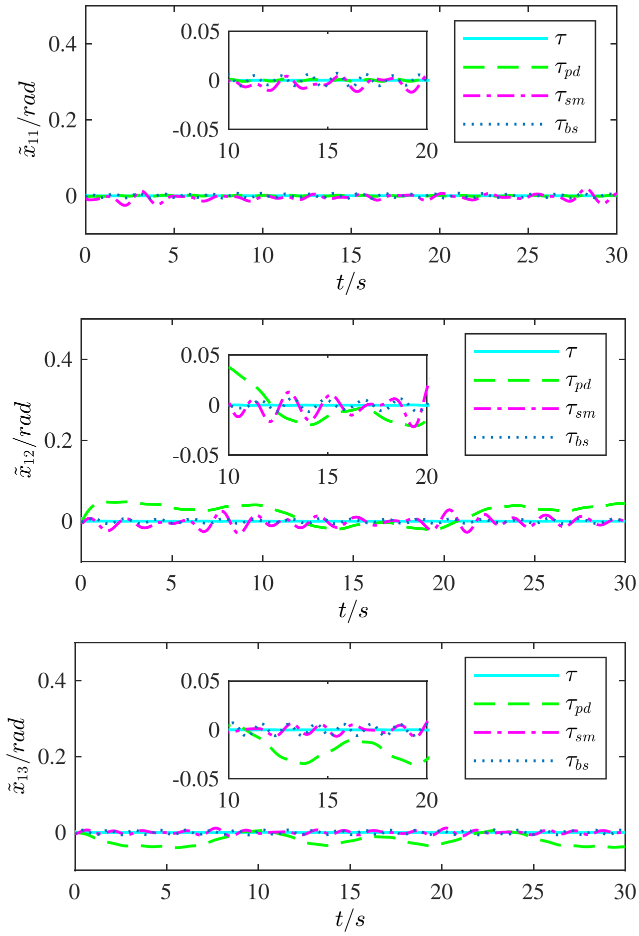

FIGURE 4. Joint position tracking errors under scenario 1.

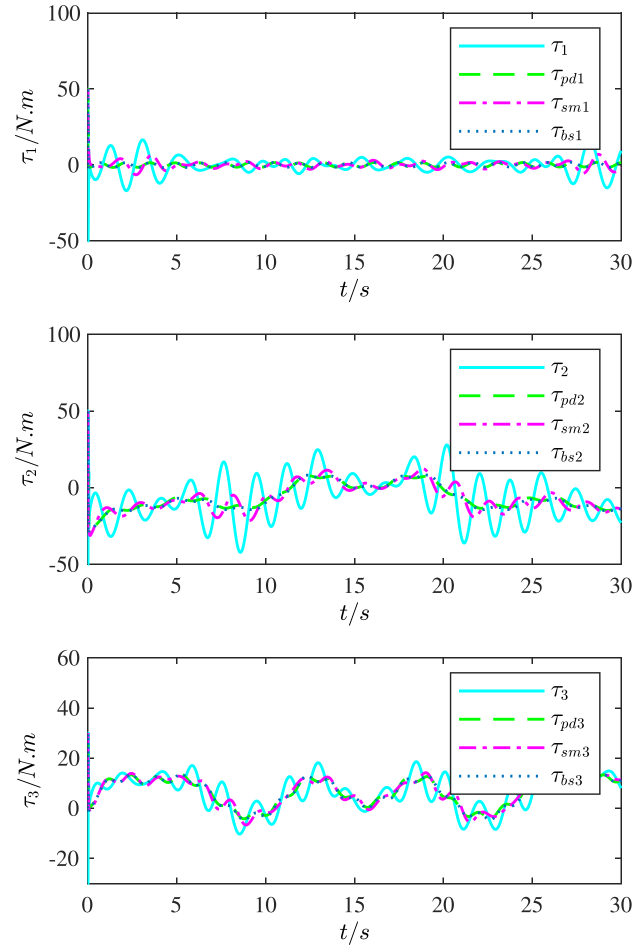

FIGURE 5. Control effort of the different controllers under scenario 1.

We choose desired trajectories, unknown time-varying mismatched disturbances as

$$x_d = [x_{d1}, x_{d2}, x_{d3}]^T = \begin{bmatrix} 1.5\sin(0.2t) \\ 1.5\sin(0.1t) \\ 1.5\sin(0.5t) \end{bmatrix}, \quad (64)$$

$$d(t) = [d_1, d_2, d_3]^{\mathrm{T}} = \begin{bmatrix} \cos(2.5t) - 2\cos(3.5t) \\ 2\cos(3.5t) - \sin(2.5t) \\ \sin(2.5t) + 2\cos(3.5t) \end{bmatrix}. \quad (65)$$

Figure 2 show the estimation of the mismatched disturbances. It is obviously shown that the MDO can quickly track unknown mismatched disturbances. We design three scenarios to illustrate performance of the proposed controller.

A. TRACKING WITH SMALL EXTERNAL DISTURBANCES

In the first simulation, the following small time-varying disturbances

$$\tau_d = [\tau_{d1}, \tau_{d2}, \tau_{d3}]^{\mathrm{T}} = \begin{bmatrix} 1.5\cos(4.5t) \\ 1.5\sin(3.5t) \\ 1.5\sin(4.5t) \end{bmatrix} \quad (66)$$

was applied. The position tracking performance of joints 1-3 under the controllers are shown in Figure 3. Figure 4 shows

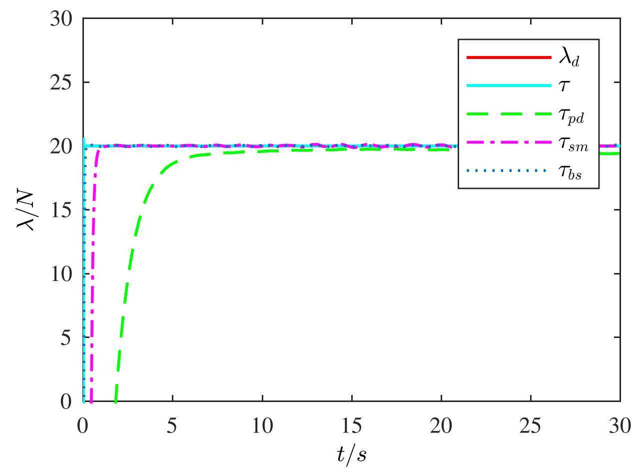

FIGURE 6. Interaction force tracking under scenario 1.

the position tracking errors. Observing Figures 3 and 4, we notice that all four controllers are capable of swiftly tracking the desired signal. However, the PD controller exhibits the poorest tracking performance when small disturbances occur. In contrast, the SMC controller outperforms the PD

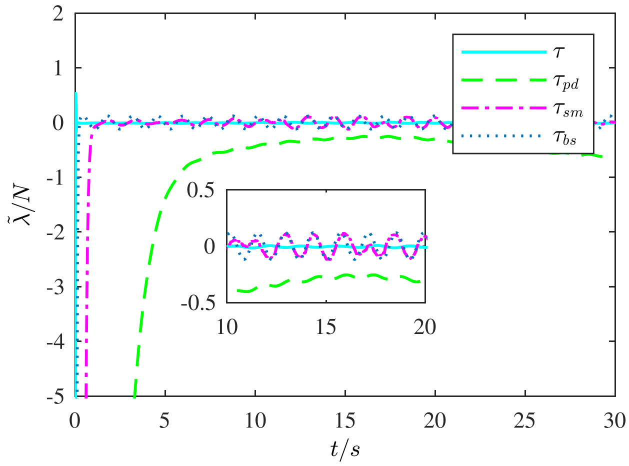

FIGURE 7. Force tracking errors under scenario 1.

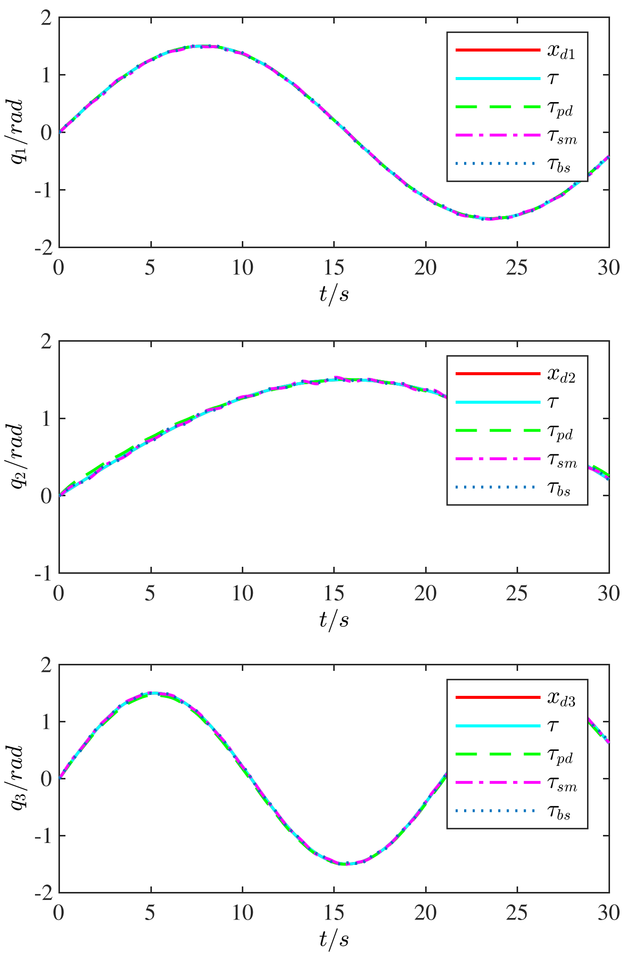

FIGURE 8. The tracking performance comparison under scenario 2.

controller in terms of tracking performance. Notably, both the ARHFPC and Back-stepping controllers demonstrate superior performance. The control efforts exerted by each joint for the controllers are depicted in Figure 5, indicating that the proposed ARHFPC controller provides continuous

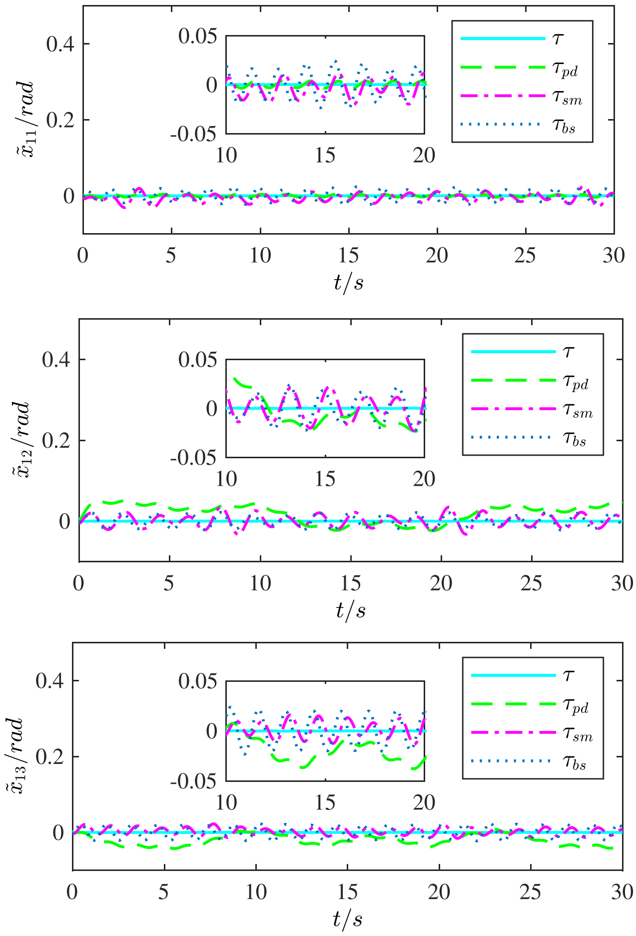

FIGURE 9. Joint position tracking errors under scenario 2.

control input. Figure 6 and Figure 7 show the interaction force tracking and tracking errors. Combining Figure 3 to Figure 7, based on the proposed controller, we can obtain that it has minor tracking errors and better control performance when the system is affected by small disturbances.

B. TRACKING WITH LARGE EXTERNAL DISTURBANCES

A large time-varying disturbances

$$\tau_d = [\tau_{d1}, \tau_{d2}, \tau_{d3}]^{\mathrm{T}} = \begin{bmatrix} 5\cos(4.5t) \\ 5\sin(3.5t) \\ 5\sin(4.5t) \end{bmatrix} \tag{67}$$

are applied to the system. It is clear that the large time-varying disturbances has an enormous influence on the performance of four controllers. Figure 8-Figure 9 show position tracking performance and tracking errors. Figure 11-Figure 12 show force tracking performance and tracking errors, respectively. According to the above figures, the PD and SMC offer worse force and position tracking performance. The benefits of the NN term compensation are significant in conditions where the large time-varying disturbances exist. Low steady-state errors and fast transient response are provided by the ARHFPC. In addition, it also provides a continuous control

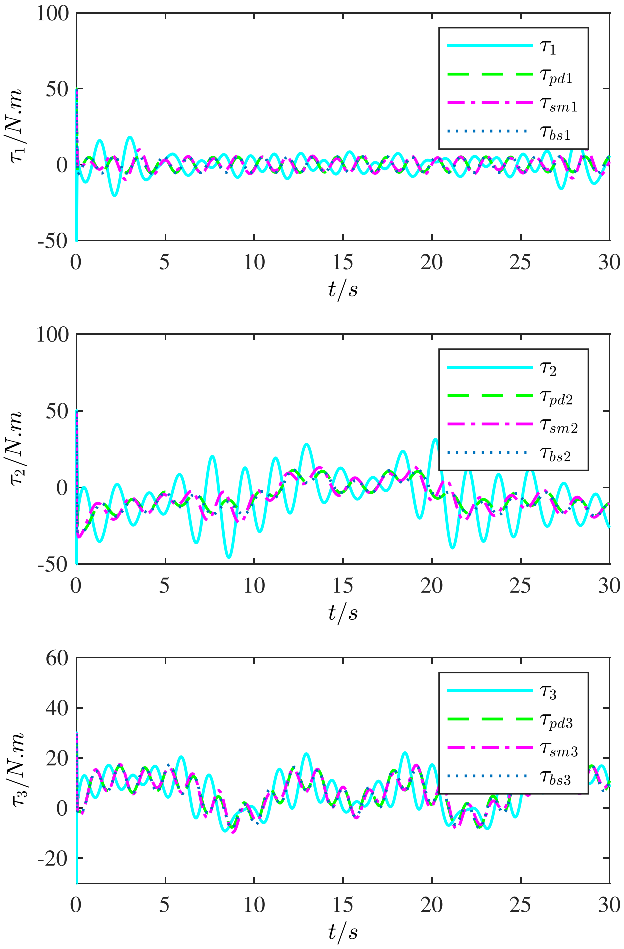

FIGURE 10. Control effort of the different controllers under scenario 2.

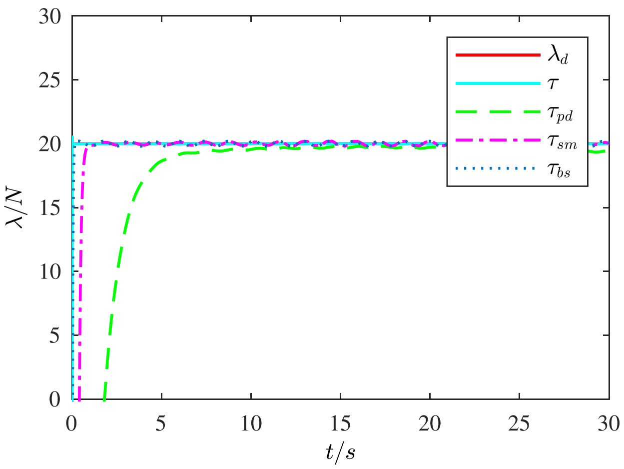

FIGURE 11. Interaction force tracking under scenario 2.

input from Figure 10. The proposed controller still maintains good control performance, and the tracking errors can meet the actual expectation.

C. TRACKING WITH DYNAMIC UNCERTAINTIES

This scenario is designed to illustrate the robustness of the ARHFPC controller by considering the dynamic

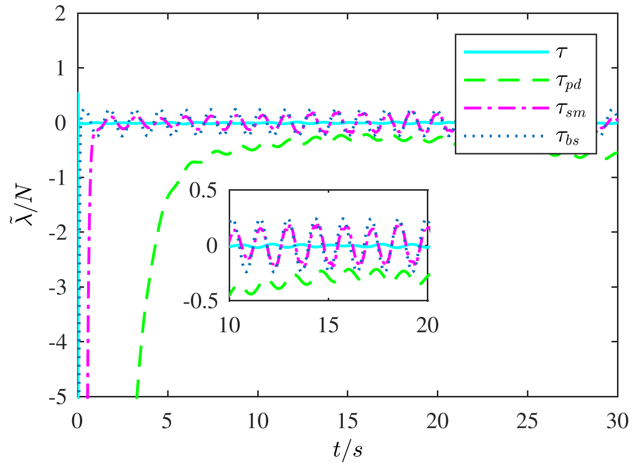

FIGURE 12. Force tracking errors under scenario 2.

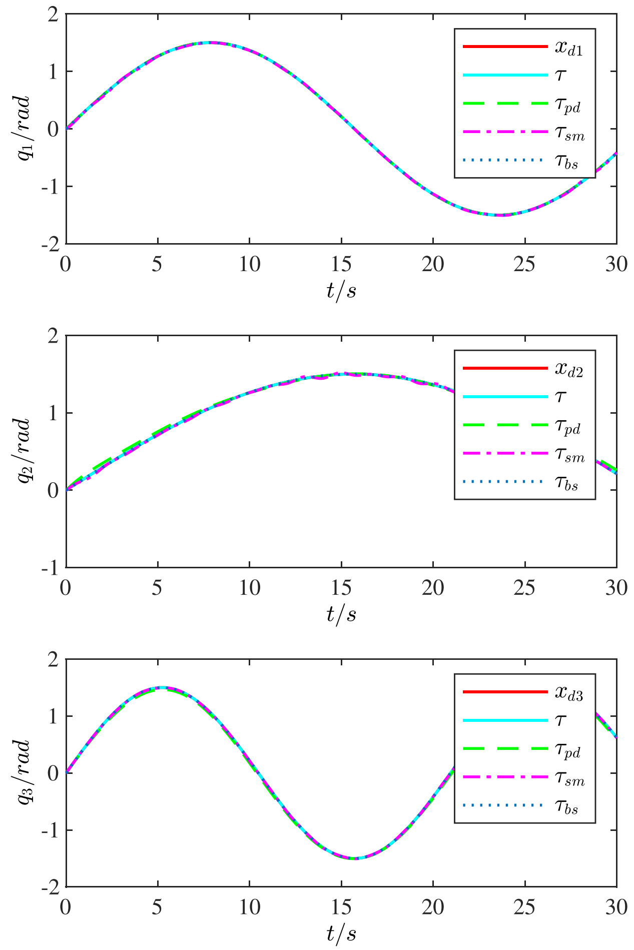

FIGURE 13. The tracking performance comparison under scenario 3.

uncertainties. The uncertainties terms are selected as: $\Delta M = 0.4M$, $\Delta C = 0.5C$, $\Delta G = 0.2G$. Figure 13 to Figure 14 clearly demonstrate that the proposed ARHFPC controller is still has good tracking accuracy for the desired position. The proposed ARHFPC controller also provides a continuous

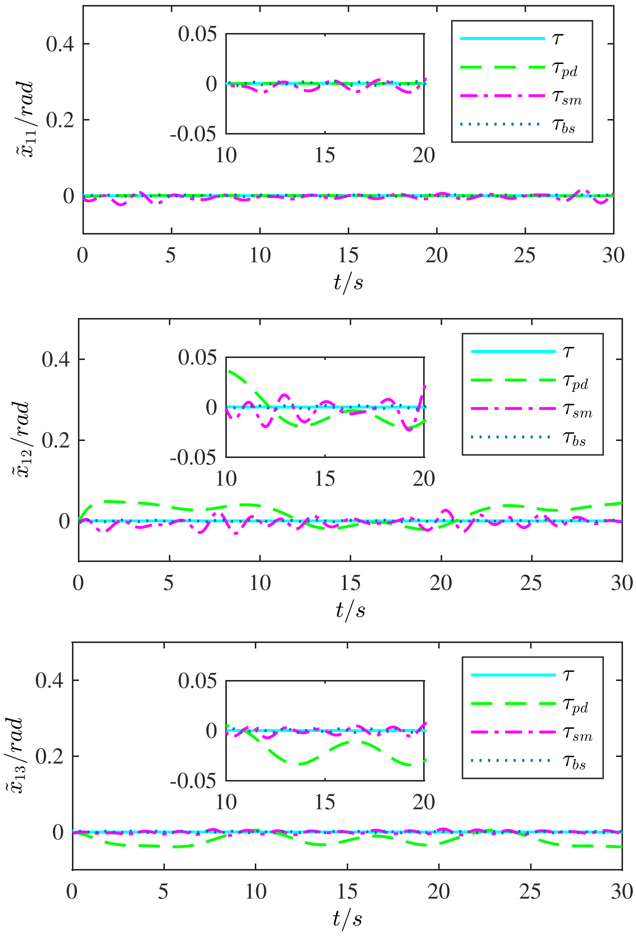

FIGURE 14. Joint position tracking errors under scenario 3.

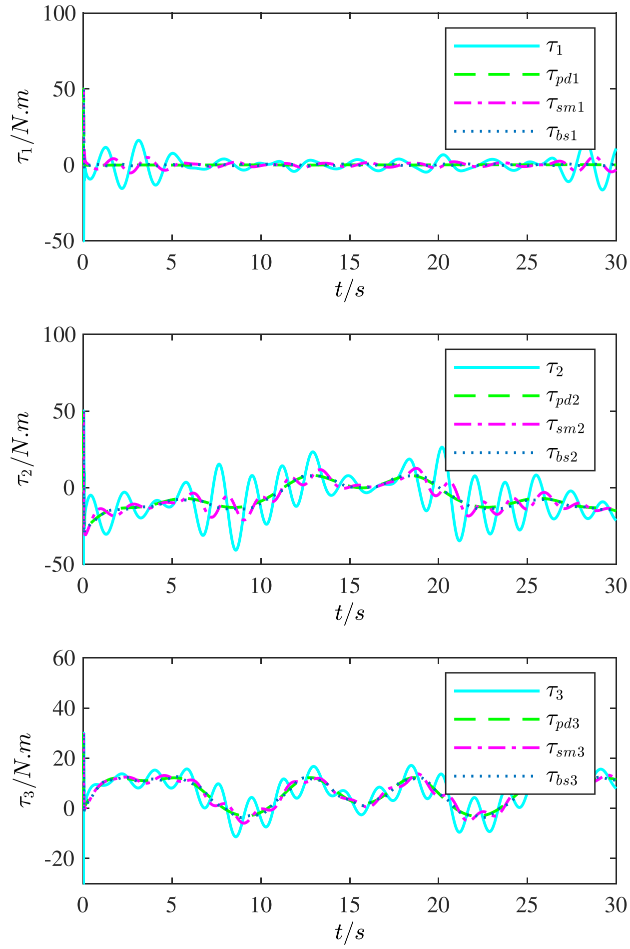

FIGURE 15. Control effort of the different controllers under scenario 3.

TABLE 4. Comparison results of performance indices.

Controller	scenario 1	scenario 2	scenario 3
τ	0.0683	0.0731	0.0672
τ_{pd}	0.8517	0.8843	0.8426
τ_{sm}	0.5642	0.6192	0.5573
τ_{bs}	0.2232	0.2819	0.1945

control input from Figure 15. Figure 16 to Figure 17 show that the force tracking performance is also well guaranteed. The updating process of the adaptive of RBFNN weights is given in Figure 18.

For the purpose of comparing the results of the above controllers, the tracking errors is quantified by considering the following performance indices are proposed as following

$$I_{RSE} = \frac{1}{N}\sum_{i=1}^{N}\sqrt{\|e_1(k)\|^2+\|e_2(k)\|^2+\|e_3(k)\|^2+\left\|\tilde{\lambda}(k)\right\|^2}, \tag{68}$$

where $e_i, i = 1, 2, 3$ is the tracking error of three joints. And the comparison results are drawn in Table 4.

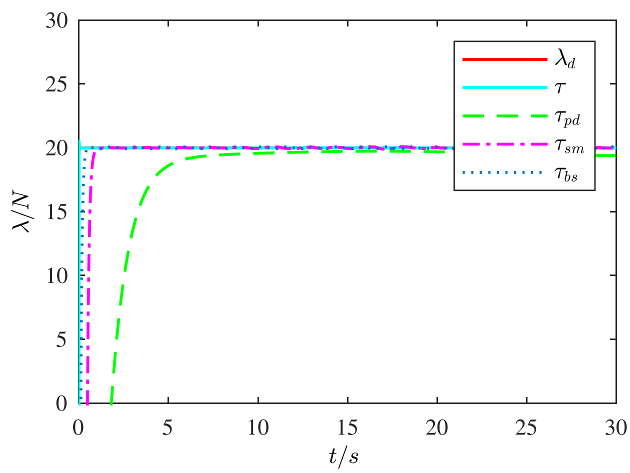

FIGURE 16. Interaction force tracking under scenario 3.

From Table 4, it is evident that the proposed controller achieves smaller indices in all scenarios, indicating superior control performance. This improvement can be attributed to the introduced MDO and NN terms compensations,

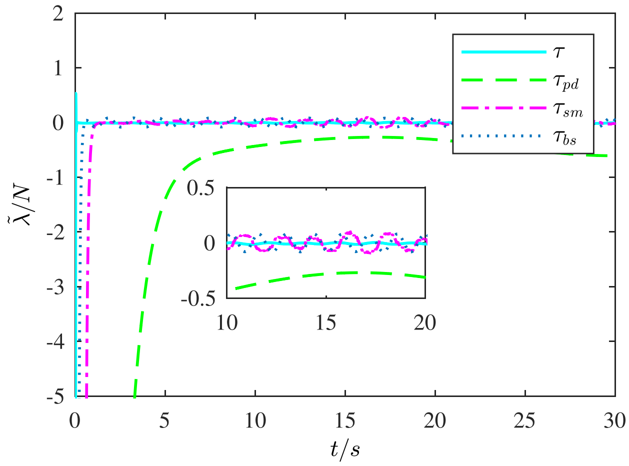

FIGURE 17. Force tracking errors under scenario 3.

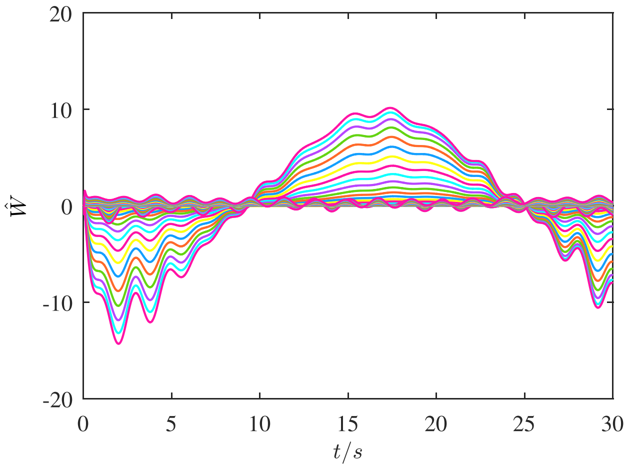

FIGURE 18. The updating process of the adaptive of RBFNN weights.

facilitating the rapid convergence of estimated mismatched disturbances and uncertainties towards their actual values.

Overall, the proposed ARHFPC controller demonstrates the best performance in terms of steady-state error, transient response, force, and position tracking accuracy, as evident from the comparison results provided above.

VI. CONCLUSION

The main objective is to address the hybrid force/position control problem for robot manipulators subject to dynamic uncertainties, matched and mismatcheded disturbances, and input saturation. Firstly, the position controller is developed using backstepping technique. Then, the first-order low-pass filter and the ADS are synthesized into the controller to overcome the virtual control's complex derivative operation and handle the input saturation effect, respectively. Additionally, the force controller for the end-effector's interaction with the environment is enhanced using Fuzzy Proportional-Integral (FPI) control. Due to the approximation capacity of the RBFNNs, it is utilized to compensate for the effects of matched disturbances, joint friction and dynamic uncertainties. External disturbances consist of matched and unmatched disturbances. Since the robot manipulators are impacted by numerous disturbances during operation that reduce the system control performance, an observer is designed specifically for the mismatched disturbances, aiming to improve control accuracy by accurately estimating these disturbances and mitigating their effects on the system states. It can provide that all the control signals of the whole system are asymptotically stable by Lyapunov stable theroy. The proposed approach achieves better tracking performance in terms of matched and mismatched disturbance rejection, uncertainties and input saturation. It indicates the best performance in terms of steady state error, transient response, force and positions tracking accuracy from the above comparison results. The limitations of the proposed method are that the matched and mismatcheded disturbances are assumed to be continuously conductible. For future work, we will investigate the influences of sensor faults on the system and make a compensation for it in the course of operation.

APPENDIX

LIST OF ABBREVIATIONS

ADS	Auxiliary Dynamic System.
ARHFPC	Adaptive Robust Hybrid Force/Position Control.
FIS	Fuzzy Inference System.
FPI	Fuzzy Proportional-Integral.
MDO	Mismatched Disturbance Observer.
RBFNNs	Radial Basis Function Neural Networks.
SMC	Sliding Mode Control.
UUB	Uniformly Ultimately Bounded.

LIST OF SYMBOLS

$\tau = [\tau_1, \cdots, \tau_n]^{\mathrm{T}}$	Actual input vector.
$\tau_d = [\tau_{d1}, \cdots, \tau_{dn}]^{\mathrm{T}}$	Matched disturbance vector.
$C(q, \dot{q})$	Coriolis and Centrifugal force matrix.
$d(t) = [d_1, \cdots, d_n]^{\mathrm{T}}$	Unknown time-varying mismatched disturbances.
$F_f(\dot{q}) = \left[F_{f1}, \cdots, F_{fn}\right]^{\mathrm{T}}$	Joint friction vector.
$G(q)$	Gravitation torque.
J	Jacobian matrix.
$M(q)$	Inertia matrix.
$q, \dot{q}, \ddot{q}$	Positions, velocities, and accelerations vectors.

REFERENCES

[1] L. Jin, S. Li, J. Yu, and J. He, "Robot manipulator control using neural networks: A survey," *Neurocomputing*, vol. 285, pp. 23–34, Apr. 2018.

[2] S. Haddadin, A. De Luca, and A. Albu-Schäffer, "Robot collisions: A survey on detection, isolation, and identification," *IEEE Trans. Robot.*, vol. 33, no. 6, pp. 1292–1312, Dec. 2017.

[3] W. He, Y. Dong, and C. Sun, "Adaptive neural impedance control of a robotic manipulator with input saturation," *IEEE Trans. Syst., Man, Cybern., Syst.*, vol. 46, no. 3, pp. 334–344, Mar. 2016.

[4] W. He, Y. Chen, and Z. Yin, "Adaptive neural network control of an uncertain robot with full-state constraints," *IEEE Trans. Cybern.*, vol. 46, no. 3, pp. 620–629, Mar. 2016.

[5] J. Chen, C. Lin, B. Chen, and Z. Zhang, "Observer-based adaptive neural control for a class of nonlinear singular systems," *Int. J. Robust Nonlinear Control*, vol. 30, no. 10, pp. 4043–4058, Jul. 2020.

[6] J. Chen, J. Yu, and H.-K. Lam, "New admissibility and admissibilization criteria for nonlinear discrete-time singular systems by switched fuzzy models," *IEEE Trans. Cybern.*, vol. 52, no. 9, pp. 9240–9250, Sep. 2022.

[7] H. Chaudhary, V. Panwar, R. Prasad, and N. Sukavanam, "Adaptive neuro fuzzy based hybrid force/position control for an industrial robot manipulator," *J. Intell. Manuf.*, vol. 27, no. 6, pp. 1299–1308, Dec. 2016.

[8] D. M. Tuan and P. D. Hieu, "Adaptive position/force control for robot manipulators using force and velocity observer," *J. Electr. Eng. Technol.*, vol. 14, no. 6, pp. 2575–2582, Nov. 2019.

[9] E. Lutscher, E. C. Dean-León, and G. Cheng, "Hierarchical force and positioning task specification for indirect force controlled robots," *IEEE Trans. Robot.*, vol. 34, no. 1, pp. 280–286, Feb. 2018.

[10] Z. Wang, L. Zou, X. Su, G. Luo, R. Li, and Y. Huang, "Hybrid force/position control in workspace of robotic manipulator in uncertain environments based on adaptive fuzzy control," *Robot. Auto. Syst.*, vol. 145, Nov. 2021, Art. no. 103870.

[11] H. Navvabi and A. H. D. Markazi, "Hybrid position/force control of stewart manipulator using extended adaptive fuzzy sliding mode controller (E-AFSMC)," *ISA Trans.*, vol. 88, pp. 280–295, May 2019.

[12] C. Cao, F. Wang, Q. Cao, H. Sun, W. Xu, and M. Cui, "Neural network–based terminal sliding mode applied to position/force adaptive control for constrained robotic manipulators," *Adv. Mech. Eng.*, vol. 10, no. 6, 2018.

[13] S. Xu, B. He, Y. Zhou, Z. Wang, and C. Zhang, "A hybrid position/force control method for a continuum robot with robotic and environmental compliance," *IEEE Access*, vol. 7, pp. 100467–100479, 2019.

[14] A. Karamali Ravandi, E. Khanmirza, and K. Daneshjou, "Hybrid force/position control of robotic arms manipulating in uncertain environments based on adaptive fuzzy sliding mode control," *Appl. Soft Comput.*, vol. 70, pp. 864–874, Sep. 2018.

[15] J. Peng, S. Ding, Z. Yang, and F. Zhang, "Neural network-based hybrid position/force tracking control for robotic systems without velocity measurement," *Neural Process. Lett.*, vol. 51, no. 2, pp. 1125–1144, Apr. 2020.

[16] J. Peng, Z. Yang, Y. Wang, F. Zhang, and Y. Liu, "Robust adaptive motion/force control scheme for crawler-type mobile manipulator with nonholonomic constraint based on sliding mode control approach," *ISA Trans.*, vol. 92, pp. 166–179, Sep. 2019.

[17] Z. Yang, J. Peng, and Y. Liu, "Adaptive neural network force tracking impedance control for uncertain robotic manipulator based on nonlinear velocity observer," *Neurocomputing*, vol. 331, pp. 263–280, Feb. 2019.

[18] J. Yang, S. Li, and X. Yu, "Sliding-mode control for systems with mismatched uncertainties via a disturbance observer," *IEEE Trans. Ind. Electron.*, vol. 60, no. 1, pp. 160–169, Jan. 2013.

[19] H. Min, S. Xu, B. Zhang, and N. Duan, "Practically finite-time control for nonlinear systems with mismatching conditions and application to a robot system," *IEEE Trans. Syst., Man, Cybern., Syst.*, vol. 50, no. 2, pp. 480–489, Feb. 2020.

[20] J. Guo, Y. Liu, C. Cheng, and J. Zhou, "Disturbance attenuation–based sliding mode control with disturbance observer for mismatched uncertain system," *Adv. Mech. Eng.*, vol. 9, no. 8, 2017.

[21] Y. Li, M. Zeng, H. An, and C. Wang, "Disturbance observer-based control for nonlinear systems subject to mismatched disturbances with application to hypersonic flight vehicles," *Int. J. Adv. Robot. Syst.*, vol. 14, no. 2, 2017.

[22] C. Lv, H. Yu, N. Zhao, J. Chi, H. Liu, and L. Li, "Robust state-error port-controlled Hamiltonian trajectory tracking control for unmanned surface vehicle with disturbance uncertainties," *Asian J. Control*, vol. 24, no. 1, pp. 320–332, Jan. 2022.

[23] H. Sun and L. Guo, "Neural network-based DOBC for a class of nonlinear systems with unmatched disturbances," *IEEE Trans. Neural Netw. Learn. Syst.*, vol. 28, no. 2, pp. 482–489, Feb. 2017.

[24] L. Liu, X. Song, Z. Fu, and S. Song, "Disturbance observer-based input-output finite-time control of a class of nonlinear systems," *Math. Problems Eng.*, vol. 2017, pp. 245–256, Jan. 2017.

[25] H. Zhang, X. Wei, L. Zhang, and M. Tang, "Disturbance rejection for nonlinear systems with mismatched disturbances based on disturbance observer," *J. Franklin Inst.*, vol. 354, no. 11, pp. 4404–4424, Jul. 2017.

[26] E. Kayacan and T. I. Fossen, "Feedback linearization control for systems with mismatched uncertainties via disturbance observers," *Asian J. Control*, vol. 21, no. 3, pp. 1064–1076, May 2019.

[27] X. Fang, F. Liu, Z. Wang, and N. Dong, "Novel disturbance-observer-based control for systems with high-order mismatched disturbances," *Int. J. Syst. Sci.*, vol. 49, no. 2, pp. 371–382, Jan. 2018.

[28] D. G. Nguyen, D. T. Tran, and K. K. Ahn, "Disturbance observer-based chattering-attenuated terminal sliding mode control for nonlinear systems subject to matched and mismatched disturbances," *Appl. Sci.*, vol. 11, no. 17, p. 8158, Sep. 2021.

[29] Z. Guo, J. Guo, X. Wang, J. Chang, and H. Huang, "Sliding mode control for systems subjected to unmatched disturbances/unknown control direction and its application," *Int. J. Robust Nonlinear Control*, vol. 31, no. 4, pp. 1303–1323, Mar. 2021.

[30] X. Liu, D. Liu, and H. Sheng, "Position tracking control of robotic system subject to matched and mismatched disturbances," *Math. Problems Eng.*, vol. 2020, pp. 1–11, Sep. 2020.

[31] C. Zhou, C. Dai, J. Yang, and S. Li, "Disturbance observer-based tracking control with prescribed performance specifications for a class of nonlinear systems subject to mismatched disturbances," *Asian J. Control*, vol. 25, no. 1, pp. 359–370, Jan. 2023.

[32] C. Makkar, G. Hu, W. G. Sawyer, and W. E. Dixon, "Lyapunov-based tracking control in the presence of uncertain nonlinear parameterizable friction," *IEEE Trans. Autom. Control*, vol. 52, no. 10, pp. 1988–1994, Oct. 2007.

[33] C. Lv, H. Yu, J. Chen, N. Zhao, and J. Chi, "Trajectory tracking control for unmanned surface vessel with input saturation and disturbances via robust state error IDA-PBC approach," *J. Franklin Inst.*, vol. 359, no. 5, pp. 1899–1924, Mar. 2022.

[34] B. Armstrong, O. Khatib, and J. Burdick, "The explicit dynamic model and inertial parameters of the Puma 560 arm," in *Proc. IEEE Int. Conf. Robot. Autom.*, Apr. 1986, pp. 510–518.

CHENGXING LV received the B.Sc. degree in automation and the M.Sc. degree in control theory and control engineering from Qufu Normal University, China, in 2005 and 2008, respectively, and the Ph.D. degree in system theory from Qingdao University, China, in 2019. He is currently an Associate Professor with the School of Information and Control Engineering, Qingdao University of Technology, Qingdao, China. His research interests include underactuated surface vessels, intelligent systems, and nonlinear control.

GANG CHEN received the B.Sc. degree in automation from Qingdao University of Technology, Qingdao, China, in 2022, where he is currently pursuing the master's degree with the School of Information and Control Engineering. His research interests include underactuated surface vessels, intelligent systems, and nonlinear control.

HUAMIN ZHAO received the M.Sc. degree in automation from Qingdao University of Technology, Qingdao, China, in 2022, and the Graduate degree from the School of Information and Control Engineering, Qingdao University of Technology. His research interests include underactuated surface vessels, intelligent systems, and nonlinear control.

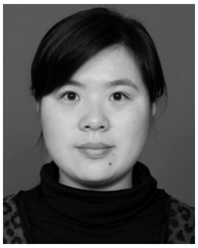

JIAN CHEN received the B.Sc. degree in mathematics from Dalian University of Technology, Dalian, China, in 2001, the M.Sc. degree in system engineering from Shandong University, Jinan, China, in 2005, and the Ph.D. degree in system theory from the Institute of Complexity Science, Qingdao University, Qingdao, China, in 2017. She is currently an Associate Professor with the School of Information and Control Engineering, Qingdao University of Technology, Qingdao. Her research interests include analysis and fuzzy control for complex nonlinear systems.

HAISHENG YU was born in Jilin, China, in 1963. He received the B.S. degree in electrical automation from Harbin University of Civil Engineering and Architecture, in 1985, the M.S. degree in computer applications from Tsinghua University, in 1988, and the Ph.D. degree in control science and engineering from Shandong University, China, in 2006. He is currently a Professor with the School of Automation Engineering, Qingdao University, China. His research interests include electrical energy conversion and motor control, applied nonlinear control, computer control, and intelligent systems.